PROCEEDINGS B

Research

Check for updates

Author for correspondence:
Robert W. Boessenecker
e-mail: boesseneckerrw@cofc.edu

THE ROYAL SOCIETY
PUBLISHING

A toothless dwarf dolphin (Odontoceti: Xenorophidae) points to explosive feeding diversification of modern whales (Neoceti)

Robert W. Boessenecker[1,2], Danielle Fraser[3], Morgan Churchill[4,5] and Jonathan H. Geisler[4]

[1]Department of Geology and Environmental Geosciences, College of Charleston, Charleston, SC 29424, USA
[2]University of California Museum of Paleontology, University of California, Berkeley, CA 94720, USA
[3]Palaeobiology, Canadian Museum of Nature, PO Box 3443 Stn 'D', Ottawa, Ontario, Canada K1P 6P4
[4]Department of Anatomy, College of Osteopathic Medicine, New York Institute of Technology, Old Westbury, NY 11568, USA
[5]Department of Biology, University of Wisconsin Oshkosh, Oshkosh, WI 54901, USA

RWB, 0000-0002-6117-128X

Toothed whales (Odontoceti) are adapted for catching prey underwater and possess some of the most derived feeding specializations of all mammals, including the loss of milk teeth (monophyodonty), high tooth count (polydonty), and the loss of discrete tooth classes (homodonty). Many extant odontocetes possess some combination of short, broad rostra, reduced tooth counts, fleshy lips, and enlarged hyoid bones—all adaptations for suction feeding upon fishes and squid. We report a new fossil odontocete from the Oligocene (approx. 30 Ma) of South Carolina (*Inermorostrum xenops*, gen. et sp. nov.) that possesses adaptations for suction feeding: toothlessness and a shortened rostrum (brevirostry). Enlarged foramina on the rostrum suggest the presence of enlarged lips or perhaps vibrissae. Phylogenetic analysis firmly places *Inermorostrum* within the Xenorophidae, an early diverging odontocete clade typified by long-snouted, heterodont dolphins. *Inermorostrum* is the earliest obligate suction feeder within the Odontoceti, a feeding mode that independently evolved several times within the clade. Analysis of macroevolutionary trends in rostral shape indicate stabilizing selection around an optimum rostral shape over the course of odontocete evolution, and a post-Eocene explosion in feeding morphology, heralding the diversity of feeding behaviour among modern Odontoceti.

1. Introduction

The Oligocene represents one of the most important periods of whale evolution, with fossils documenting the initial diversification of toothed whales (Odontoceti) and baleen whales (Mysticeti) from ancestral Eocene archaeocetes [1–3]. Whereas the middle to late Eocene is characterized by low cetacean diversity (10–12 genera), the Oligocene is characterized by a rapid rise in diversity that culminates in more than 40 Chattian genera [2, fig. 7.1]. Nearly all middle and late Eocene archaeocetes are generalized marine hunters that use raptorial feeding to capture prey, and share similarities in dentition and rostral shape [3,4]. By contrast, Oligocene cetaceans display a wide array of rostral shapes and tooth morphologies. Morphological diversity has been studied most intensely across Mysticeti, which achieved maximum morphological disparity in the Oligocene [5], possibly spurred by the development of the circum-Antarctic current and the associated increase in upwelling and productivity [6]. Oligocene mysticetes include raptorial feeders (*Fucaia*, *Janjucetus*; [7,8]), suction-based benthic feeders (*Mammalodon*; [9]), and baleen-based filter feeders (Aetiocetidae, Eomysticetidae, *Llanocetus*; [10,11]). Additional studies have shown that the early Oligocene is not only a key time for Mysticeti [5,6], but for Neoceti (baleen and toothed whales) as a whole [12,13].

Far less attention has been given to the diversification of Oligocene odontocetes. Most described Oligocene odontocetes are, like archaeocetes, probable raptorial pierce feeders. However, they possess specialized features including longer rostra and, in some cases, tusk-like upper and lower incisors [14,15]. One Oligocene odontocete, *Simocetus rayi*, lacks premaxillary teeth, and possesses a downturned rostrum, which has been used to infer benthic suction feeding [16]. However the full ecological diversity of Oligocene odontocetes remains poorly known, in part because only a small number of fossil taxa have been fully described [2,12].

Here we report a diminutive, short-snouted, toothless xenorophid dolphin, *Inermorostrum xenops*, from the lower Oligocene Ashley Formation of South Carolina. *Inermorostrum xenops* is an aberrant species because it represents only the eleventh documented evolutionary loss of maxillary teeth among all mammals (six of those occur within Cetacea [17]), and has the shortest maxilla of all known extant and extinct cetaceans. *Inermorostrum* further expands the known morphological diversity of cetaceans during the early Oligocene, prompting a re-evaluation of neocete diversification.

2. Material and methods

Inermorostrum xenops was added into a recently published comprehensive cladistic matrix for Oligocene whales [18,19] containing 88 terminal taxa, 308 morphological characters [20], and 60 851 molecular characters [21,22], to investigate its phylogenetic placement. Although it could only be scored for 95 characters (30.8% of the morphological partition), we were able to confidently place *Inermorostrum* within the phylogeny (see *Phylogeny and evolution of feeding morphology*). Phylogenetic analyses were performed in TNT v.1.1 using default settings and both equal and implied weighting ($k = 3$) under a new technology search. Support for nodes in the weighted ($k = 3$) and unweighted trees was assessed using 100 bootstrap replicates with replacement, as implemented in TNT [23]. Default values and selections were used except as follows: (i) absolute frequencies instead of frequency differences were used, and (ii) shortest trees for each replicate were found using 50, not 10, random taxon addition sequences followed by tree bisection-reconnection swapping.

To examine the evolution of rostral length, we calculated the rostral proportion index (RPI) by dividing length of the rostral portion of the maxilla by the width of the rostrum at the antorbital notch. Measurements were recorded from published photographs using IMAGEJ, measured directly from specimens, and, in a few cases, taken directly from published measurements (electronic supplementary material, Information S2). The RPI is correlated with the mandibular bluntness index [24], but focuses on the maxillary portion of the rostrum. We chose RPI instead of length of the mandible or the total rostrum because it is measurable for the largest number of fossil taxa; most fossil species are represented by specimens preserving part of the rostrum or mandibles, although odontocete mandibles are often incomplete.

We time scaled the strict consensus trees from both the equal and implied weighting analyses using the CAL3 method [25]. Taxa for which RPI values were not available were pruned from the trees, limiting analyses to 60 taxa from across the odontocete phylogeny. Time scaling was based on binned first and last occurrence data (electronic supplementary material, Information S2), as implemented in the R package PALEOTREE [25]. Sampling, speciation and extinction rates for use in CAL3 were estimated using likelihood models of the observed taxon duration frequencies. Terminal occurrence dates were stochastically sampled from a uniform distribution. We generated 1000 age

calibrated trees for use in downstream macroevolutionary analyses and ancestral character state reconstruction.

To determine the mode of RPI evolution, we used the fitContinous function in the geiger R package [26] to fit models of continuous trait evolution. We fit the following models: (i) Brownian motion or random walk [27], (ii) Ornstein Uhlenbeck (OU; stabilizing selection or evolution toward an optimum) [28], and (iii) early burst (EB; decelerating evolutionary rate or accelerating-decelerating) [29,30]. We adjusted the bounds of the OU and EB models to improve parameter estimation via maximum likelihood (electronic supplementary material, Information S3). We ran the OU model using various starting parameter values for α (strength of the pull toward the optimum) and σ^2 (Brownian motion rate parameter) and high numbers of maximum-likelihood iterations (1000–10 000) to improve our confidence in the parameter estimates (results not shown). All models were fit to the entire posterior distribution of dated trees for both the weighted and unweighted strict consensus phylogenies (2000 trees). We therefore generated a posterior distribution of parameter estimates and sample-size corrected Akaike information criterion (AICc) values, which were averaged for summary purposes. We do not interpret the reconstructed root state for the OU model because, in a single optimum OU model as is fitted here, θ (also called μ) or the optimum trait value cannot be estimated separately from the root state. In a single optimum OU model, the root state is therefore assumed to be equal to θ [31].

Ancestral character state reconstruction (ACSR) of RPI was performed using a maximum-likelihood approach in the phytools R package [32]. As with fitContinous, ACSR was performed across the entire posterior distribution of dated trees for both the weighted and unweighted strict consensus phylogenies (2000 trees). We chose the evolutionary model based on the outcome of the macroevolutionary analyses, as described above. We reconstructed ancestral states for all nodes in all trees (electronic supplementary material, Information S4) and took the average. All R code used for CAL3 tree dating, model fitting, and ACSR can be found in the electronic supplementary material, Information S3.

We observed no major differences in the overall trends we report for ACSR and evolutionary model fitting when we performed CAL3 tip dating setting anc.wt = 0 (no allowance for inferring ancestor-descendent relationships) and therefore do not present the results herein.

Institutional abbreviations: CCNHM, College of Charleston Mace Brown Museum of Natural History, College of Charleston, Charleston, SC 29424; ChM, The Charleston Museum, Charleston, SC 29424.

3. Systematic palaeontology

Inermorostrum xenops gen. et sp. nov.

Etymology. The generic name is from the Latin *inermus*, meaning weapon-less or defenceless, and *rostrum*, meaning snout, referring to the absence of teeth in the rostrum. The species name derives from Greek for strange, *xeno*, and face, *ops*, referring to the highly derived facial morphology of the holotype.

Holotype. CCNHM 171, a partial skull consisting of the maxillary portion of the rostrum, portions forming the nasal passages, most of the orbital region, and the frontal portion of the intertemporal constriction.

Type locality and horizon. Collected by A. Allen, C. Hoyle, and M. Schnarr *ex situ* from the Wando River, Berkeley County, South Carolina. Adhering limestone matrix with coral (*Balanophyllia* sp.) is consistent with derivation from the Lower Oligocene Ashley Formation. Subsurface deposits

3

of the Ashley Formation near the Wando River have been mapped as the Runnymede Marl Member (29.0–28.75 Ma) of the Ashley Formation [33], although assignment to member is tentative because the Ashley Formation in this area is poorly studied.

Referred specimen. ChM PV5258, fragment of braincase including ascending process of premaxilla, nasals, and frontals collected *in situ* from the Givhans Ferry Member of the Ashley Formation by Matthew Swilp, December 1986.

Diagnosis. Inermorostrum xenops differs from all other Odontoceti (except some Ziphiidae and Physeteridae, *Australodelphis*, *Grampus*, *Monodon*, and *Odobenocetops*) in having a completely toothless maxilla and rostral portion of the maxilla shorter than 50% postorbital skull width. *Inermorostrum xenops* shares with other Xenorophidae, to the exclusion of all other odontocetes, several features including: (i) nasal process of premaxilla extending posteriorly to contact frontal and excluding maxilla from frontal contact; (ii) nasal process of premaxilla underlying ascending maxilla; (iii) premaxilla with lateral crest adjacent to the bony nares; (iv) large antorbital fossa on rostral portion of maxilla; (v) lacrimal expanded over the orbit; and (vi) frontal window posterior to orbit exposing premaxilla in ventral view. *Inermorostrum xenops* differs from all other Xenorophidae in possessing an anteroposteriorly short, toothless maxilla, and further differs from *Cotylocara* and *Echovenator* in lacking a deep postnarial fossa.

4. Morphology and body size

Inermorostrum xenops is distinguished by a short, triangular, and rapidly tapering rostrum with a faintly convex palate (figure 1). The maxilla is nearly complete and, though damaged anteriorly, approximately 11 mm is missing from the anterior tip of the right maxilla (electronic supplementary material, Information S1). When scaled to antorbital width, the maxilla of *Inermorostrum* (maxilla length = 119% antorbital width) is approximately one third the length of the maxilla of *Cotylocara macei* (maxilla length = 305.2% antorbital width). In cross-section, the rostrum is much transversely wider ventrally; the palate is nearly flattened, and completely lacks teeth, alveoli, or even an alveolar groove. *Inermorostrum xenops* possesses a relatively short snout (RPI = 1.19) in comparison to other Xenorophidae (RPI = 2.52–3.34), representing one of the shortest snouts of any odontocete and the most brevirostrine Oligocene odontocete, surpassed in RPI only by mammalodontid mysticetes. We cannot rule out the presence of premaxillary or mandibular teeth. However, premaxillary teeth seem unlikely given the probable feeding ecology of *Inermorostrum* (see below) and mandibular teeth are unlikely given the lack of maxillary embrasure pits that receive the apices of the lower teeth in other xenorophids [18,34]. A complete description is presented in the electronic supplementary material, Information S1.

Inermorostrum xenops was similar in size to harbour porpoises (*Phocoena*), making it the smallest known Oligocene odontocete (estimated postorbital width = 130 mm). It is 54% the size of *Cotylocara macei* (postorbital width = 240 mm), whereas other xenorophids such as *Echovenator* (postorbital width = 160 mm) and *Albertocetus* (postorbital width = 166 mm) are somewhat smaller than *Cotylocara* but still larger than *Inermorostrum*. The median frontal suture is unfused,

perhaps indicating the holotype was immature. However, the median frontal suture is fused in the referred specimen ChM PV5258 which is of similar size to CCNHM 171. Furthermore, the premaxilla-maxilla suture is partially closed, indicating that the rostrum had attained adult proportions. Thus, the small size and short rostrum of *Inermorostrum* cannot be simply attributed to ontogenetic immaturity.

5. Feeding ecology

Feeding in aquatic environments presents unique challenges. Odontocetes have evolved two strategies to capture prey and transfer it to into the back of the mouth [35–37]. Raptorial feeding, which is plesiomorphic for Neoceti, involves capturing prey with teeth and then using movements of the mandible to work prey towards the back of the mouth [36,38]. Gular suction feeding requires a rapid increase in the volume of the oral cavity, usually induced by contraction of hyoid musculature, and use of the lips to form a small opening through which water and prey can enter the mouth [37–41]. Raptorial and suction-feeding behaviours are not mutually exclusive, and species may use a combination of both to capture a particular prey item [24,38,41]; suction-feeding specialists probably evolve from raptorial ancestors [38].

Even though suction-feeding involves structures that do not fossilize (i.e. the lips, tongue, and hyoid muscles), it can be inferred from the presence of osteological correlates. Feeding experiments indicate that odontocetes with short rostra (e.g. *Globicephala*, *Kogia*) frequently capture prey using gular suction, and that a short, wide rostrum facilitates the formation of a small, circular oral opening [24,36,37,39,41]. Tooth reduction may enhance suction by reducing obstructions in the oral opening or result from the abandonment of a raptorial feeding strategy. Suction-feeding taxa that retain anterior teeth often have reduced anterior teeth that barely emerge above the gingiva [40,41]. More importantly, species that have few to no teeth all appear to be obligate suction-feeders [24]. Two extant suction-feeding taxa, ziphiids and *Physeter*, are differentiated from other suction-feeders by having long rostra [24]. Further, in ziphiids, *Physeter*, and *Monodon*, the teeth may be retained only for social [24] or sensory purposes [42]. To summarize, taxa with long rostra and teeth may or may not suction-feed, whereas taxa with short rostra and no maxillary teeth are obligate suction-feeders [24,36,41]. Thus the extremely short rostrum in *Inermorostrum* and the absence of maxillary teeth is strong evidence that it was a suction-feeder.

Xenorophid dolphins with well-preserved crania exhibit ventrally deflected rostra; in *Cotylocara macei* the rostrum is deflected 20° relative to the basicranial stem [34]. Xenorophids such as *Cotylocara* and *Echovenator* are the earliest echolocating odontocetes [18,34,43]; the dense bone of the interorbital shield may have reflected sounds forward without interference from the ventrally deflected rostrum. Though incomplete, the rostrum of the holotype of *Inermorostrum xenops* deviates approximately 20° from the anterior basicranial stem (presphenoid), similar to *Cotylocara*. Ventrally deflected rostra in modern and extinct sirenians is correlated with benthic feeding [44]. A ventrally deflected rostrum in *Inermorostrum xenops* and other xenorophids may therefore suggest benthic feeding. Similarly, the strange odontocete *Simocetus rayi* exhibits a deflected rostrum that has been interpreted as an adaptation
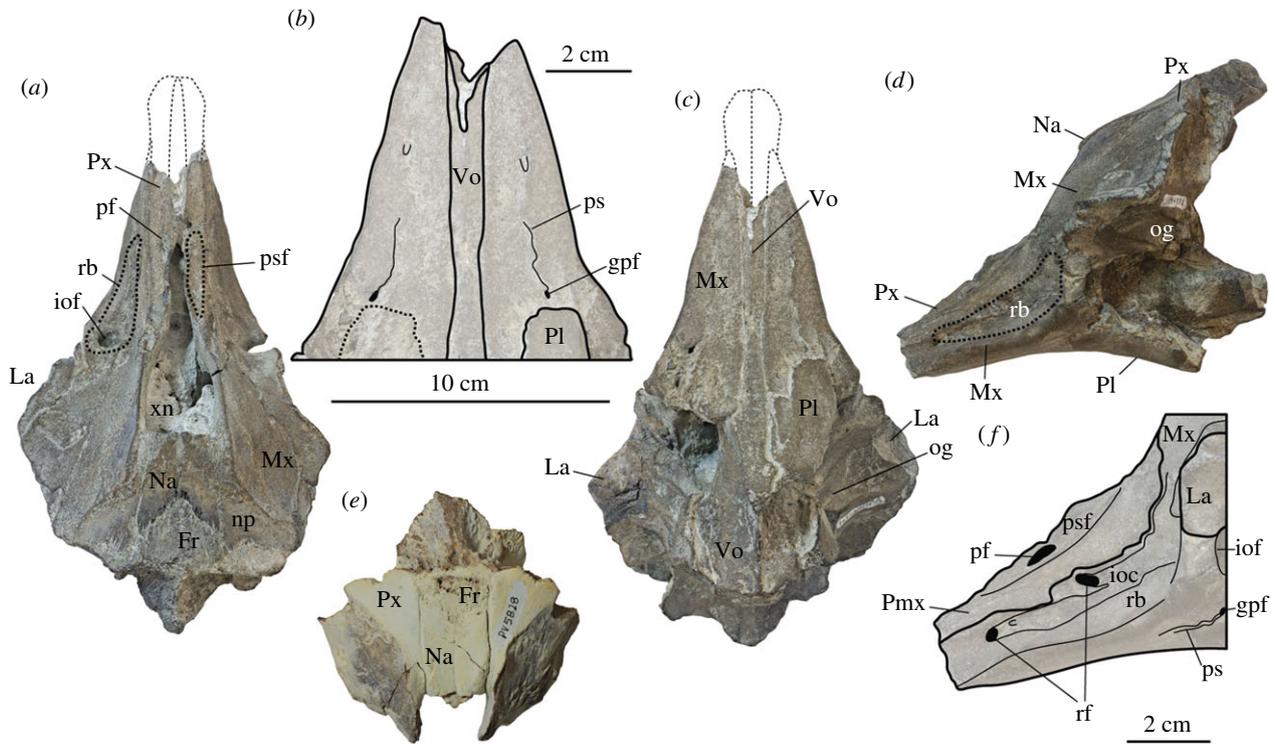
Figure 1. Holotype cranium in (*a*) dorsal, (*b*) palate in ventral, (*c*) ventral, (*d*) lateral, (*f*) rostrum in lateral, and (*e*) referred specimen in dorsal view. Fr, frontal; gpf, greater palatine foramen; ioc, infraorbital canal; iof, infraorbital foramen; La, lacrimal; Mx, maxilla; Na, nasal; np, nasal process of premaxilla; og, optic groove; Pl, palatine; pf, premaxillary foramen; ps, palatine sulcus; psf, premaxillary sac fossa; Px, premaxilla; rb, rostral basin; rf, reentrant foramina; Vo, vomer; xn, external nares.

for benthic foraging [16]. The small adult body size of *Inermorostrum* would inhibit deep diving capability as in extant cetaceans [45], thus suggesting shallower diving consistent with benthic feeding.

Other anatomical aspects of *I. xenops* may be suggestive of ecological specialization. The infraorbital foramen is of similar proportion to *Cotylocara*, even though the rostrum is much smaller in size; when scaled to rostrum length, the infraorbital foramen of *Inermorostrum* measures 16.8% of rostrum length as opposed to 5% in *Cotylocara*. The infra-orbital foramen in *Inermorostrum* further differs from most Odontoceti by leading to a deeply entrenched, anteriorly-extending, branching sulcus with several enlarged foramina. The most anterior foramen might be homologous to the inci-sivomaxillary canal. Homologous foramina are present in *Cotylocara*, but are proportionally and absolutely smaller than in *Inermorostrum* (despite the larger size of *Cotylocara*), and restricted to the posteriormost rostral basin [34]. In dogs, the infraorbital foramen transmits the superior alveolar nerve and arteries, and the lateral and dorsal nasal arteries [46]. Because the former innervate and provide blood to the upper dentition, such an enlarged bony conduit in a toothless taxon is unexpected. Although speculative, the large infraorbital canal and associated sulci may suggest the presence of large fleshy lips and/or vibrissae [47]. In terrestrial mammals the lateral rostral artery supplies the epidermis that bears facial vibrissae [46]. In the benthic suction-feeding walrus *Odobenus rosmarus*, an enlarged infraorbital canal transmits a similarly enlarged maxillary branch of the trigeminal nerve which innervates the mystacial pad and vibrissae [48]. Furthermore, modified vibrissae in extant odontocetes act as electroreceptors and have been linked with benthic feeding behaviour [49] as proposed herein for *Inermorostrum*.

6. Phylogeny and evolution of feeding morphology

In both phylogenetic analyses (electronic supplementary material, Information S1), *Inermorostrum* is embedded within the Xenorophidae, the earliest diverging clade within Odontoceti [18,34,50]. *Inermorostrum* exhibits one synapo-morphy of this clade: maxilla wedged between palatines. A more exclusive clade (Xenorophidae *sensu* [19]) consists of *Albertocetus meffordorum*, *Cotylocara macei*, *Echovenator sandersi*, *I. xenops*, *Xenorophus* spp., and several unnamed xenorophids (ChM PV 4746, 4834, 5711). *Inermorostrum* preserves four syna-pomorphies of this clade: (i) ventral exposure of lacrimojugal that is intermediate in size; (ii) loss of infraborbital plate; (iii) premaxilla wedged between frontal and maxilla and overlapping frontal; and (iv) nasal process of premaxilla pachyostotic. *Inermorostrum* is sister to a clade including *Cotylocara*, *Echovenator*, and unnamed xenorophid repre-sented by ChM PV 2758; one synapomorphy unites *Inermorostrum* and other members of this clade: ventromedial edge of ventral infraorbital foramen formed exclusively by the maxilla.

Based on our phylogenetic hypothesis, brevirostry and longirostry have evolved in parallel among different odonto-cete clades (figure 2, electronic supplementary material, Information S1); see also [24]). Brevirostry has evolved numerous times within Odontoceti (figure 2), including within Xenorophidae (*Inermorostrum*), ?Squalodontidae (*Prosqualodon*), ?Eurhinodelphinidae (*Vanbreenia*), Ponto-poriidae (*Protophocaena*), Physeteroidea (*Kogia*), and within Delphinoidea (*Odobenocetops*, Monodontidae, Phocoenidae, *Cephalorhynchus*, *Orcinus*, Globicephalinae). Longirostry evolved at least four times within odontocetes, including
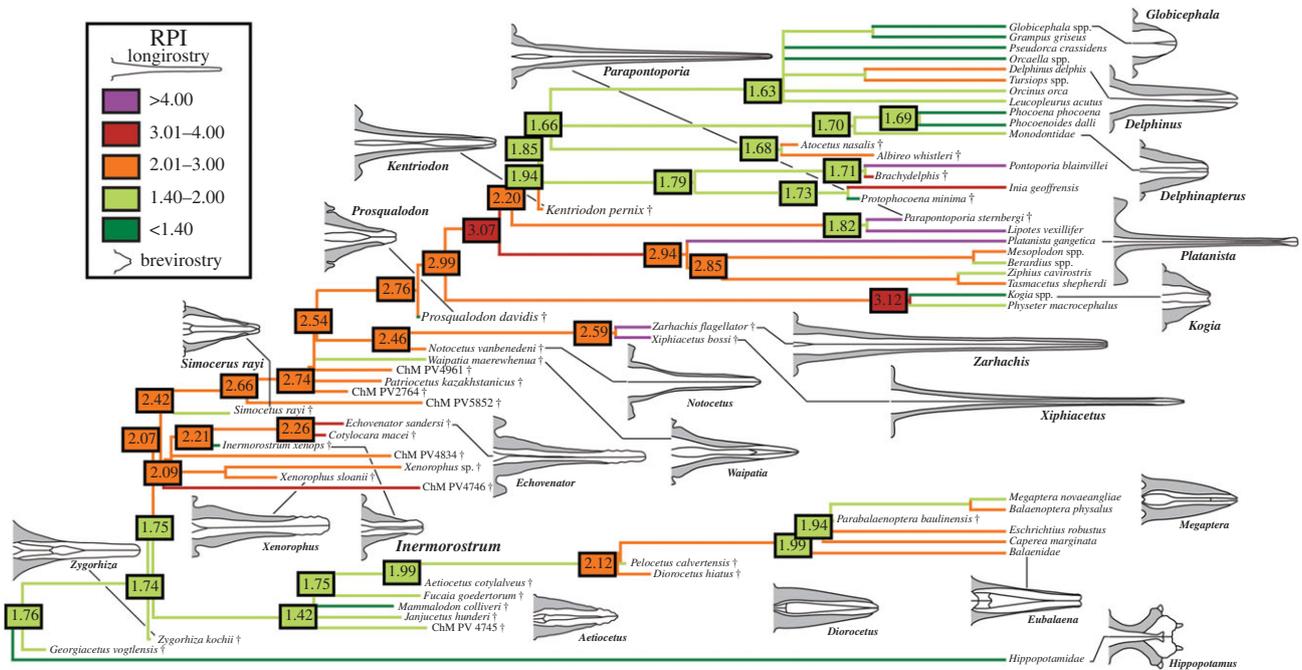
Figure 2. Phylogenetic relationships of *Inermorostrum* with ancestral state reconstruction for rostral proportions. Phylogeny represents the strict consensus from the equal weighting phylogenetic analysis. Taxa and nodes are colour coded by RPI value. Skulls reduced to same antorbital width with maxilla in grey. Single strict consensus tree pruned to include only taxa with rostral measurements.

Table 1. Summary of evolutionary model fits to the (*a*) weighted and (*b*) unweighted consensus trees. (Model fitting was performed across a posterior distribution of 1000 dated trees for both the unweighted and weighted phylogenies for a total of 2000 fitted models. Best fit models are italicized.)

	model	ΔAICc	AICc	σ^2	α	r	root state
(*a*)	Brownian	1.24	200.90	0.17	—	—	1.68
	Ornstein–Uhlenbeck	*0.00*	*199.67*	*0.33*	*0.07*	*—*	*2.43*
	early burst (ACDC)	1.35	201.01	0.10	—	0.02	1.71
(*b*)	*Brownian*	*0.00*	*196.92*	*0.17*	*—*	*—*	*1.68*
	Ornstein–Uhlenbeck	*0.01*	*196.93*	*0.30*	*0.05*	*—*	*2.32*
	early burst (ACDC)	0.72	197.64	0.11	—	0.02	1.70

within Xenorophidae (*Echovenator*, *Cotylocara*, and ChM PV4746), Eurhinodelphinidae, Platanistidae, and Inioidea.

The ancestral RPI for Odontoceti (approx. 2.07) is higher than the ancestral cetacean condition (1.76). The majority of nodes along the odontocete 'backbone' consistently exhibit reconstructed values ranging from 1.8–3, suggesting an optimum rostrum length within Odontoceti (figure 2; electronic supplementary material, Information S1). Exceptions include Delphinoidea, and possibly Delphinida as reconstructed using the posterior distribution of dated trees from the weighted phylogeny. We find further support for an optimal rostrum length using macroevolutionary analyses fitted to the posterior distribution of dated trees from the weighted phylogeny (table 1*a*), which identified the OU model of stabilizing selection as best fit to RPI using AICc; rostral length fluctuated within a given optimum range, and probably experienced no radical shifts in selection since the Oligocene. Evolutionary model fitting identified the Brownian motion and OU models as equally good fits to the posterior distribution of dated trees from the unweighted strict consensus phylogeny (table 1*b*). Differences in model fit between the weighted and unweighted phylogenies probably

relate to the differences in overall phylogenetic resolution as well as placement of Lipotidae and *Kentriodon* between the two analyses.

Analysis of cetacean rostral proportions through the Cainozoic (middle Eocene-Holocene; figure 3) indicates that *Inermorostrum*, which is Rupelian in age, is one of the earliest brevirostrine odontocetes. Prior to the Rupelian, the variation of RPI of Priabonian cetaceans is very low (1.15–1.68). With the exception of the Remingtonocetidae (3.43), low diversity of rostral shape characterizes all Eocene cetaceans. The Rupelian also marks an increase in the maximum RPI, which continued to increase until it peaked in the early Miocene (Burdigalian). Thereafter, the maximum RPI gradually decreases, but continues to be relatively high (e.g. extant *Platanista*). By contrast, minimum RPI for odontocetes appears to have stabilized earlier with the appearance of *Inermorostrum*, with a ratio of approximately 0.8–1.2. The RPI of *Inermorostrum* is slightly lower than that observed in Mysticeti and archaeocetes. However, the difference between brevirostrine odontocetes and archaeocetes plus mysticetes is even greater if total rostral length is considered (i.e. premaxilla and maxilla). We speculate that the minimum RPI
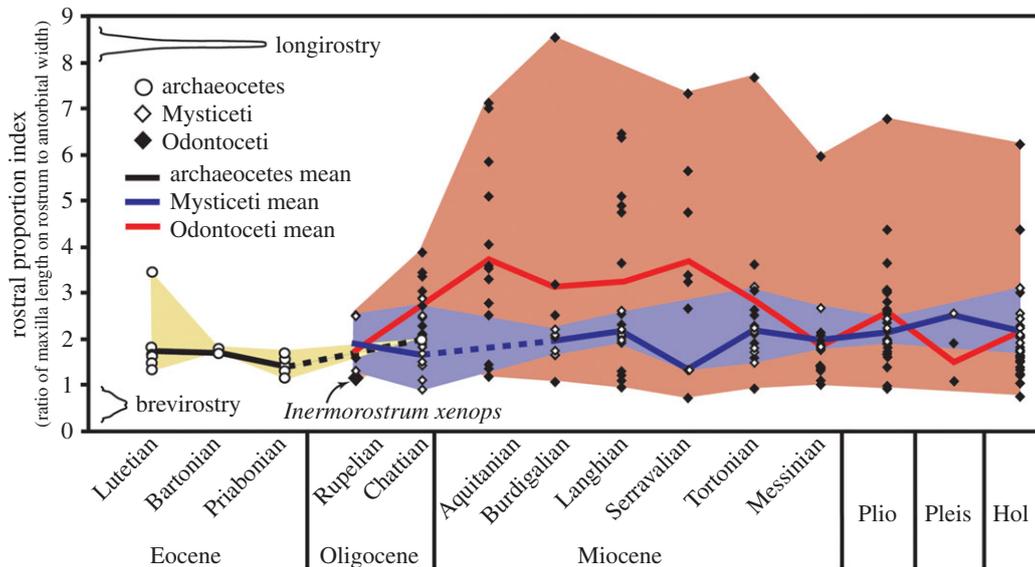
Figure 3. Trends in RPI among cetaceans through the Cainozoic. See the electronic supplementary material, Information S2 for measurements.

observed in odontocetes is constrained by the presence of a melon and associated facial musculature, common to all extant Odontoceti and inferred to occur in all known extinct odontocetes [34]. Suction-feeding pilot and dwarf/pygmy sperm whales (*Globicephala*, *Kogia*) are among the most extreme extant brevirostrine cetaceans (RPI = 1.25–0.74), and their enlarged melon slightly overhangs the short rostrum. Longirostry (high RPI) is poorly studied among cetaceans but convergence between longirostrine crocodiles (gharials) and river dolphins is related to a diet including small fishes, and perhaps relates to rapid lateral snapping (sweep feeding) [51].

The oldest known odontocetes (Rupelian in age) have a mean RPI (figure 3) similar to that of archaeocetes (approx. 1.75). However, the mean RPI for Odontoceti increases during the early and middle Miocene (3.0–3.5) and decreases thereafter during the middle and late Miocene (3.0–1.5). Mean RPI for Mysticeti (1.5–2.5) is generally similar to that of archaeocetes throughout their history with a slight increase after the late Miocene (figure 3).

7. Discussion

A proportionally short rostrum and absence of maxillary teeth strongly indicate that *I. xenops* was one of the earliest obligate suction-feeders in Cetacea. *Inermorostrum* is also remarkable for its small size and large infraorbital foramen suggestive of specialized, facial soft tissues. A recent study [35] hypothesized that the ability to suction-feed is probably primitive for Neoceti based on a Bayesian optimization of behaviour and morphology on a consensus phylogeny. Their results are heavily influenced by the fact that some cetaceans, like *Eschrichtius*, can suction-feed despite lacking obvious osteological adaptations. The discovery of a suction-feeding specialist within the earliest diverging odontocete clade (Xenorophidae) supports this hypothesis [35].

Inermorostrum is one of the earliest occurring fossil odontocetes and indicates that, within four million years of the appearance of Neoceti, highly derived ecological specializations typical of extant odontocetes had already evolved from the basilosaurid bauplan. Recent discoveries of

Oligocene Neoceti with specialized feeding adaptations, including *Inermorostrum*, *Simocetus*, *Janjucetus*, *Mammalodon*, *Aetiocetus*, and *Waharoa* [7,9–11,16], further suggest that the early radiation of Neoceti was driven by diversification in feeding ecology. We show herein that the odontocete RPI envelope rapidly expands from the Rupelian to the Burdigalian (figure 3), tracking extreme longirostry in certain lineages (e.g. *Prepomatodelphis*, *Zarhachis*) and brevirostry in others (e.g. *Inermorostrum*, *Prosqualodon*). The range in rostral proportions for Mysticeti circumscribes a rather narrow envelope (figure 3), suggestive of morphological conservatism, perhaps constrained by filter feeding.

Why did the radiation in feeding morphology occur with the origin of Neoceti, nearly 15 million years after cetaceans first invaded aquatic environments? One possible explanation is that diversification was driven by increases in primary productivity that resulted from the late Eocene initiation of the circum Antarctic current, a hypothesis that has been used to explain the early rostral diversity of basal mysticetes [5,6]. The rapid radiation of whales in the Oligocene may also be related to the development of a key evolutionary novelty at the base of Neoceti, possibly the loss of tooth replacement [1,52]. It is tempting to suggest that loss of tooth replacement facilitated the parallel evolution of rostral shape, dental simplification, and polydonty within Odontoceti and Neoceti [53]. Whether the Neocete radiation that led to the evolution of *Inermorostrum* and other taxa resulted from environment-independent changes in regulatory genes or changes in ocean circulation and productivity will require a much better understanding of the palaeoecology of early fossil neocetes as well as the genetic linkages, if any, among the unique and unusual features of the cetacean feeding apparatus.

7

rspb.royalsocietypublishing.org Proc. R. Soc. B 284: 20170531

References

1. Gatesy J, Geisler JH, Chang J, Buell C, Berta A, Meredith RW, Springer MS, McGowen MR. 2013 A phylogenetic blueprint for a modern whale. *Mol. Phylogenet. Evol.* **66**, 479–506. (doi:10.1016/j.ympev.2012.10.012)

2. Marx FG, Lambert O, Uhen MD. 2016 *Cetacean paleobiology.* Oxford, UK: Wiley Blackwell.

3. Uhen MD. 2004 Form, function, and anatomy of *Dorudon atrox* (Mammalia, Cetacea): an archaeocete from the middle to late Eocene of Egypt. *Univ. Mich. Pap. Paleontol.* **34**, 1–222.

4. Fahlke JM, Bastl KA, Semprebon GM, Gingerich PD. 2013 Paleoecology of archaeocete whales throughout the Eocene: dietary adaptations revealed by microwear analysis. *Palaeogeogr. Palaeoclimatol. Palaeoecol.* **386**, 690–701. (doi:10.1016/j.palaeo.2013.06.032)

5. Marx FG, Fordyce RE. 2015 Baleen boom and bust: a synthesis of mysticete phylogeny, diversity and disparity. *R. Soc. open sci.* **2**, 140434. (doi:10.1098/rsos.140434)

6. Fordyce RE. 1977 The development of the circum-Antarctic current and the evolution of the *Mysticeti* (Mammalia: Cetacea). *Palaeogeogr. Palaeoclimatol. Palaeoecol.* **21**, 265–271. (doi:10.1016/0031-0182(77)90038-4)

7. Fitzgerald EMG. 2006 A bizarre new toothed mysticete (Cetacea) from Australia and the early evolution of baleen whales. *Proc. R. Soc. B* **273**, 2955–2963. (doi:10.1098/rspb.2006.3664)

8. Marx FG, Tsai C-H, Fordyce RE. 2015 A new early Oligocene toothed 'baleen' whale (Mysticeti: Aetiocetidae) from western North America: one of the oldest and the smallest. *R. Soc. open sci.* **2**, 150476. (doi:10.1098/rsos.150476)

9. Fitzgerald EMG. 2010 The morphology and systematics of *Mammalodon colliveri* (Cetacea: Mysticeti), a toothed mysticete from the Oligocene of Australia. *Zool. J. Linn. Soc.* **158**, 367–476. (doi:10.1111/j.1096-3642.2009.00572.x)

10. Boessenecker RW, Fordyce RE. 2015 Anatomy, feeding ecology, and ontogeny of a transitional baleen whale: a new genus and species of Eomysticetidae (Mammalia: Cetacea) from the Oligocene of New Zealand. *PeerJ* **3**, e1129. (doi:10.7717/peerj.1129)

11. Deméré TA, McGowen MR, Berta A, Gatesy J. 2008 Morphological and molecular evidence for a stepwise evolutionary transition from teeth to baleen in mysticete whales. *Syst. Biol.* **57**, 15–37. (doi:10.1080/10635150701884632)

12. Fordyce RE. 2003 Cetacean evolution and Eocene-Oligocene oceans revisited. In *From greenhouse to icehouse: the marine Eocene-Oligocene transition* (eds DR Prothero, LC Ivany, EA Nesbitt), pp. 154–170. New York, NY: Columbia University Press.

13. Steeman ME *et al.* 2009 Radiation of extant cetaceans driven by restructuring of the oceans. *Syst. Biol.* **58**, 573–585. (doi:10.1093/sysbio/syp060)

14. Fordyce RE. 1994 *Waipatia maerewhenua*, new genus and new species, Waipatiidae, new family, an archaic Late Oligocene dolphin (Cetacea: Odontoceti: Platanistoidea) from New Zealand. *Proc. San Diego Soc. Nat. Hist.* **29**, 147–176. (doi:10.5962/bhl.part.10662)

15. Tanaka Y, Fordyce RE. 2015 A new Oligo-Miocene dolphin from New Zealand: *Otekaikea huata* expands diversity of the early Platanistoidea. *Palaeontol. Electronica* **18**, 1–71.

16. Fordyce RE. 2002 *Simocetus rayi* (Odontoceti, Simocetidae, new family); a bizarre new archaic Oligocene dolphin from the eastern North Pacific. *Smithson. Contrib. Paleobiology* **93**, 185–222.

17. Meredith RW, Gatesy J, Murphy WJ, Ryder OA, Springer MS. 2009 Molecular decay of the tooth gene Enamelin (ENAM) mirrors the loss of enamel in the fossil record of placental mammals. *PLoS Genet.* **5**, e1000634. (doi:10.1371/journal.pgen.1000634)

18. Churchill M, Martinez-Caceres M, Muizon CD, Mnieckowski J, Geisler JH. 2016 The origin of high-frequency hearing in whales. *Curr. Biol.* **26**, 2144–2149. (doi:10.1016/j.cub.2016.06.004)

19. Sanders AE, Geisler JH. 2015 A new basal odontocete from the upper Rupelian of South Carolina, USA, with contributions to the systematics of *Xenorophus* and *Mirocetus* (Mammalia, Cetacea). *J. Vertebr. Paleontol.* **35**, e890107. (doi:10.1080/02724634.2014.890107)

20. Geisler JH, Sanders AE. 2003 Morphological evidence for the phylogeny of Cetacea. *J. Mamm. Evol.* **10**, 23–129. (doi:10.1023/A:1025552007291)

21. Geisler JH, McGowen MR, Yang G, Gatesy J. 2011 A supermatrix analysis of genomic, morphological, and paleontological data from crown Cetacea. *BMC Evol. Biol.* **11**, 1–33. (doi:10.1186/1471-2148-11-112)

22. McGowen MR, Spaulding M, Gatesy J. 2009 Divergence date estimation and a comprehensive molecular tree of extant cetaceans. *Mol. Phylogenet. Evol.* **53**, 891–906. (doi:10.1016/j.ympev.2009.08.018)

23. Goloboff PA, Farris JS, Nixon KC. 2008 TNT, a free program for phylogenetic analysis. *Cladistics* **24**, 774–786.

24. Werth AJ. 2006 Mandibular and dental variation and the evolution of suction feeding in Odontoceti. *J. Mammal.* **87**, 579–588. (doi:10.1644/05-MAMM-A-279R1.1)

25. Bapst DW. 2013 A stochastic rate-calibrated method for time-scaling phylogenies of fossil taxa.

Methods Ecol. Evol. **4**, 724–733. (doi:10.1111/2041-210X.12081)

26. Harmon LJ, Weir JT, Brock CD, Glor RE, Challenger W. 2008 GEIGER: investigating evolutionary radiations. *Bioinformatics* **24**, 129–131. (doi:10.1093/bioinformatics/btm538)

27. Felsenstein J. 1973 Maximum likelihood estimation of evolutionary trees from continuous characters. *Am. J. Hum. Genet.* **25**, 471–492.

28. Butler MA, King AA. 2004 Phylogenetic comparative analysis: a modeling approach for adaptive evolution. *Am. Nat.* **164**, 683–695. (doi:10.1086/426002)

29. Harmon LJ *et al.* 2010 Early bursts of body size and shape evolution are rare in comparative data. *Evolution* **64–8**, 2385–2396. (doi:10.1111/j.1558-5646.2010.01025.x)

30. Blomberg SP, Garland TJ, Ives AR. 2003 Testing for phylogenetic signal in comparative data: behavioral traits are more labile. *Evolution* **57**, 717–745. (doi:10.1111/j.0014-3820.2003.tb00285.x)

31. Cooper N, Thomas GH, Venditti C, Meade A, Freckleton RP. 2015 A cautionary note on the use of Ornstein Uhlenbeck models in macroevolutionary studies. *Biol. J. Linn. Soc.* **118**, 64–77. (doi:10.1111/bij.12701)

32. Revell LJ. 2012 Phytools: an R package for phylogenetic comparative biology (and other things). *Methods Ecol. Evol.* **3**, 217–223. (doi:10.1111/j.2041-210X.2011.00169.x)

33. Weems RE *et al.* 2016 Stratigraphic revision of the Cooper Group and Chandler Bridge and Edisto Formations in the coastal plain of South Carolina. *S. C. Geol.* **49**, 1–24.

34. Geisler JH, Colbert MW, Carew JL. 2014 A new fossil species supports an early origin for toothed whale echolocation. *Nature* **508**, 383–386. (doi:10.1038/nature13086)

35. Johnston C, Berta A. 2011 Comparative anatomy and evolutionary history of suction feeding in cetaceans. *Mar. Mamm. Sci.* **27**, 493–513. (doi:10.1111/j.1748-7692.2010.00420.x)

36. Werth AJ. 2000 Feeding in marine mammals. In *Feeding: form, function and evolution in tetrapod vertebrates* (ed. K Schwenk), pp. 487–526. San Diego, CA: Academic Press.

37. Werth AJ. 2000 A kinematic study of suction feeding and associated behavior in the long-finned pilot whale, *Globicephala melas* (Traill). *Mar. Mamm. Sci.* **16**, 299–314. (doi:10.1111/j.1748-7692.2000.tb00926.x)

38. Hocking DP, Marx FG, Park T, Fitzgerald EMG, Evans AR. 2017 A behavioural framework for the evolution in predatory aquatic mammals. *Proc. R. Soc. B* **284**, 20162750. (doi:10.1098/rspb.2016.2750)

39. Bloodworth B, Marshall CD. 2005 Feeding kinematics of *Kogia* and *Tursiops* (Odontoceti: Cetacea): characterization of suction and ram feeding. *J. Exp. Biol.* **208**, 3721–3730. (doi:10.1242/jeb.01807)

40. Heyning JE, Mead JG. 1996 Suction feeding in beaked whales: morphological and observational evidence. *Nat. Hist. Mus. Los Angel. Cty Contrib. Sci.* **464**, 1–12.

41. Werth AJ. 2006 Odontocete suction feeding: experimental analysis of water flow and head shape. *J. Morphol.* **267**, 1415–1428. (doi:10.1002/jmor.10486)

42. Nweeia MT *et al.* 2014 Sensory ability in the narwhal tooth organ system. *Anat. Rec.* **297**, 599–617. (doi:10.1002/ar.22886)

43. Park T, Fitzgerald EMG, Evans AR. 2016 Ultrasonic hearing and echolocation in the earliest toothed whales. *Biol. Lett.* **12**, 20160060. (doi:10.1098/rsbl.2016.0060)

44. Domning DP. 2001 Sirenians, seagrasses, and Cenozoic ecological change in the Caribbean.

45. Noren SR, Williams TM. 2000 Body size and skeletal muscle myoglobin of cetaceans: adaptations for maximizing dive duration. *Comp. Biochem. Physiol. A Mol. Integr. Physiol.* **126**, 181–191. (doi:10.1016/S1095-6433(00)00182-3)

46. Evans HE, Lahunta AD. 2013 *Miller's anatomy of the dog*, 850 p. St. Louis, MO: Saunders-Elsevier.

47. Muchlinski MN. 2008 The relationship between the infraorbital foramen, infraorbital nerve, and maxillary mechanoreception: implications for interpreting the paleoecology of fossil mammals based on infraorbital foramen size. *Anat. Rec.* **291**, 1221–1226. (doi:10.1002/ar.20742)

48. Fay FH. 1982 Ecology and biology of the Pacific Walrus, *Odobenus rosmarus divergens* Illiger. *North Am. Fauna* **74**, 1–279. (doi:10.3996/nafa.74.0001)

49. Czech-Damal NU, Liebschner A, Miersch L, Klauer G, Hanke FD, Marshall CD, Dehnhardt G, Hanke W. 2012 Electroreception in the Guiana dolphin (*Sotalia*

Palaeogeogr. Palaeoclimatol. Palaeoecol. **166**, 27–50. (doi:10.1016/S0031-0182(00)00200-5)

guianensis). *Proc. R. Soc. B* **279**, 663–668. (doi:10.1098/rspb.2011.1127)

50. Uhen MD. 2008 A new *Xenorophus*-like odontocete cetacean from the Oligocene of North Carolina and a discussion of the basal odontocete radiation. *J. Syst. Palaeontol.* **6**, 433–452. (doi:10.1017/S1477201908002472)

51. McCurry MR, Evans AR, Fitzgerald EMG, Adams JW, Clausen PD, McHenry CR. 2017 The remarkable convergence of skull shape in crocodilians and toothed whales. *Proc. R. Soc. B* **284**, 20162348. (doi:10.1098/rspb.2016.2348)

52. Uhen MD, Gingerich PD. 2001 A new genus of dorudontine archaeocete (Cetacea) from the middle-to-late Eocene of South Carolina. *Mar. Mamm. Sci.* **17**, 1–34. (doi:10.1111/j.1748-7692.2001.tb00979.x)

53. Uhen MD. 2009 Dental morphology, evolution of. In *Encyclopedia of marine mammals* (eds WF Perrin, B Würsig, JGM Thewissen), pp. 302–307, 2nd edn. Burlington, MD: Elsevier.

8

rspb.royalsocietypublishing.org *Proc. R. Soc. B* **284**: 20170531